CC-1065 Partial Structures: Enhancement of Noncovalent Affinity for DNA Minor Groove Binding through Introduction of Stabilizing Electrostatic Interactions

Dale L. Boger* and Subas M. Sakya

Department of Chemistry, Purdue University, West Lafayette, Indiana 47907

Received September 18, 1991

The preparation and DNA binding properties of $ACDPI_n$ (4–7, n = 1–4) and $TACDPI_n$ (8–10, n = 1–3) are detailed. Comparable to observations made with $CDPI_n$ (n = 1–5), $ACDPI_3$ proved to be the optimal minor groove binding agent within the $ACDPI_n$ series, and the agents exhibited a selectivity for AT- versus GC-rich DNA which is most pronounced with $ACDPI_3$. Similarly, $TACDPI_n$ (n = 1–3) exhibited a substantial AT- versus GC-rich DNA binding selectivity (n = 3, $\Delta\Delta G°$ = −2.7 to −3.5 kcal). The direct comparison of $CDPI_n$ with $ACDPI_n$ illustrated that the introduction of a C-5 amino substituent onto the peripheral face of the agent reduces the DNA binding affinity presumably through introduction of destabilizing electrostatic interactions. In contrast, the comparison with $TACDPI_n$ revealed that the introduction of a C-5 quaternary amine substantially enhanced the DNA binding affinity through introduction of stabilizing electrostatic interactions.

(+)-CC-1065 (1), an antitumor antibiotic isolated from *Streptomyces zelensis*,[1,2] has been shown to possess exceptionally potent in vitro cytotoxic activity,[3] efficacious in vivo antitumor activity,[4] and broad-spectrum antimicrobial activity.[1] The antitumor activity of 1 has been related to its sequence-selective alkylation of DNA within high affinity minor groove sites that has been demonstrated to proceed by 3′-adenine N3 alkylation of the electrophilic cyclopropane present in the left-hand subunit (CPI) of the agent.[5,6] The observation that (+)-*N*-acetyl-CPI exhibits a comparable albeit less intense (ca. 10000×) DNA alkylation within some segments of double-stranded DNA has led to the suggestion that the alkylation subunit of 1 plays the dominant role in determining the alkylation selectivity.[5] This has been further interpreted to be due to a rate-determining, sequence-dependent autocatalytic activation of the alkylation reaction by a strategically located phosphate in the DNA backbone two base-pairs removed from the alkylation site.[7] However, more recent studies have addressed an additional origin of the alkylation selectivity that may be related to the sequence-dependent conformational variability of duplex DNA.[8]

Complementary to these more recent studies, we have shown that simplified agents including $CDPI_3$ methyl ester exhibit a substantial preference for minor groove binding within AT-rich versus GC-rich DNA[9,10] attributable to the preferential stabilization of the noncovalent complex within the narrower, sterically more accessible AT-rich minor groove.[11,12] In these efforts, the profile of DNA alkylation by simple derivatives of the alkylation subunit proved to be readily distinguishable from that of (+)-CC-1065[13,14] and an autocatalytic phosphate activation of the alkylation reaction was shown not to be uniquely responsible for the alkylation selectivity.[14-16] In these studies, the electrophilic cyclopropane proved not to be obligatory to observation of the (+)-CC-1065 characteristic alkylation selectivity and the apparent noncovalent binding selectivity of the agents was shown to exhibit a pronounced effect. In the course of the continuing investigations,[17-20] we have examined the effects of the peripheral substituents on the noncovalent DNA minor groove binding affinity and selectivity of agents related to CC-1065.[9]

Herein, we report the results of a study of $ACDPI_n$ (4–7, n = 1–4) which highlight an apparent destabilizing contribution to the DNA binding affinity through introduction of a strong electronegative substituent onto the peripheral

* Address correspondence to this author at Department of Chemistry, The Scripps Research Institute, 10666 North Torrey Pines Road, La Jolla, CA 92037.

(1) Chidester, C. G.; Krueger, W. C.; Mizsak, S. A.; Duchamp, D. J.; Martin, D. G. *J. Am. Chem. Soc.* **1981**, *103*, 7629. Hanka, L.; J.; Dietz, A.; Gerpheide, S. A.; Kuentzel, S. L.; Martin, D. G. *J. Antibiot.* **1978**, *31*, 1211. Martin, D. G.; Biles, C.; Gerpheide, S. A.; Hanka, L. J.; Krueger, W. C.; McGovern, J. P.; Mizsak, S. A.; Neil, G. L.; Stewart, J. C.; Visser, J. *J. Antibiot.* **1981**, *34*, 1119.

(2) Rachelmycin, isolated from *Streptomyces* strain C-329 has been shown to be identical to CC-1065: Nettleton, D. E.; Jr.; Bush, J. A.; Bradner, W. T. U.S. Patent 4,301,248; *Chem. Abstr.* **1982**, *96*, 33362e.

(3) Bhuyan, B. K.; Newell, K. A.; Crampton, S. L.; Von Hoff, D. D. *Cancer Res.* **1982**, *42*, 3532.

(4) Martin, D. G.; Chidester, C. G.; Duchamp, D. J.; Mizsak, S. A. *J. Antibiot.* **1980**, *33*, 902.

(5) Hurley, L. H.; Reynolds, V. L.; Swenson, D. H.; Petzold, G. L.; Scahill, T. A. *Science* **1984**, *226*, 843. Reynolds, V. L.; Molineux, I. J.; Kaplan, D. J.; Swenson, D. H.; Hurley, L. H. *Biochemistry* **1985**, *24*, 6228. Hurley, L. H.; Lee, C.-S.; McGovren, J. P.; Warpehoski, M. A.; Mitchell, M. A.; Kelly R. C.; Aristoff, P. A. *Biochemistry* **1988**, *27*, 3886.

(6) For recent reviews see: Warpehoski, M. A.; Hurley, L. H. *Chem. Res. Toxicol.* **1988**, *1*, 315. Coleman, R. S.; Boger, D. L. In *Studies in Natural Products Chemistry*; Atta-ur-Rahman, Ed.; Elsevier: Amsterdam, 1989; Vol. 3, p 301. Rawal, V. H.; Jones, R. J.; Cava, M. P. *Heterocycles* **1987**, *25*, 701.

(7) Hurley, L. H.; Warpehoski, M. A.; Lee, C.-S.; McGovren, J. P.; Scahill, T. A.; Kelly, R. C.; Mitchell, M. A.; Wicnienski, N. A.; Gebhard, I.; Johnson, P. D.; Bradford, V. S. *J. Am. Chem. Soc.* **1990**, *112*, 4633. Lin, C. H.; Beale, J. M.; Hurley, L. H. *Biochemistry* **1991**, *30*, 3597.

(8) Lin, C. H.; Sun, D.; Hurley, L. H. *Chem. Res. Toxicol.* **1991**, *4*, 26. Lee, C.-S.; Sun, D.; Kizu, R.; Hurley, L. H. *Chem. Res. Toxicol.* **1991**, *4*, 203.

(9) Boger, D. L.; Invergo, B. J.; Coleman, R. S.; Zarrinmayeh, H.; Kitos, P. A.; Thompson, S. C.; Leong, T.; McLaughlin, L. W. *Chem.-Biol. Interact.* **1990**, *73*, 29.

(10) Boger, D. L.; Coleman, R. S.; Invergo, B. J. *J. Org. Chem.* **1987**, *52*, 1521.

(11) For recent reviews, see: Boger, D. L. In *Heterocycles in Bio-Organic Chemistry*; Bergman, J., Van der Plas, H. D., Simonyi, M., Eds.; Royal Society of Chemistry: Cambridge, 1991; p 103. Boger, D. L. In *Advances in Heterocyclic Natural Products Synthesis*; Pearson, W. H., Ed.; JAI Press: Greenwich, 1992; Vol. 2, pp 1–177.

(12) Dickerson, R. E. In *Structure and Methods, DNA and RNA*; Sarma, R. H., Sarma, M. H., Eds.; Adenine Press: Schenectady, NY, 1991; Vol. 3, p 1. Nelson, H. C. M.; Finch, J. T.; Luisi, B. F.; Klug, A. *Nature (London)* **1987**, *330*, 221. Coll, M.; Frederick, C. A.; Wang, A. H.-J.; Rich, A. *Proc. Natl. Acad. Sci. U.S.A.* **1987**, *84*, 8385. Coll, M.; Aymami, J.; van der Marel, G. A.; van Boom, J. H.; Rich, A.; Wang, A. H.-J. *Biochemistry* **1989**, *28*, 310.

(13) Boger, D. L.; Coleman, R. S.; Invergo, B. J.; Sakya, S. M.; Ishizaki, T.; Munk, S. A.; Zarrinmayeh, H.; Kitos, P. A.; Thompson, S. C. *J. Am. Chem. Soc.* **1990**, *112*, 4623.

(14) Boger, D. L.; Munk, S. A.; Zarrinmayeh, H.; Ishizaki, T.; Haught, J.; Bina, M. *Tetrahedron* **1991**, *47*, 2661.

(15) Boger, D. L.; Munk, S. A.; Zarrinmayeh, H. *J. Am. Chem. Soc.* **1991**, *113*, 3980.

(16) Boger, D. L.; Zarrinmayeh, H.; Munk, S. A.; Kitos, P. A.; Suntornwat, O. *Proc. Natl. Acad. Sci. U.S.A.* **1991**, *88*, 1431.

(17) Boger, D. L.; Munk, S. A.; Ishizaki, T. *J. Am. Chem. Soc.* **1991**, *113*, 2779. Boger, D. L.; Ishizaki, T. *Tetrahedron Lett.* **1990**, *31*, 793.

(18) Boger, D. L.; Ishizaki, T.; Sakya, S. M.; Munk, S. A.; Kitos, P. A.; Jin, Q.; Besterman, J. M. *BioMed. Chem. Lett.* **1991**, *1*, 115.

0022-3263/92/1957-1277$03.00/0

Scheme I

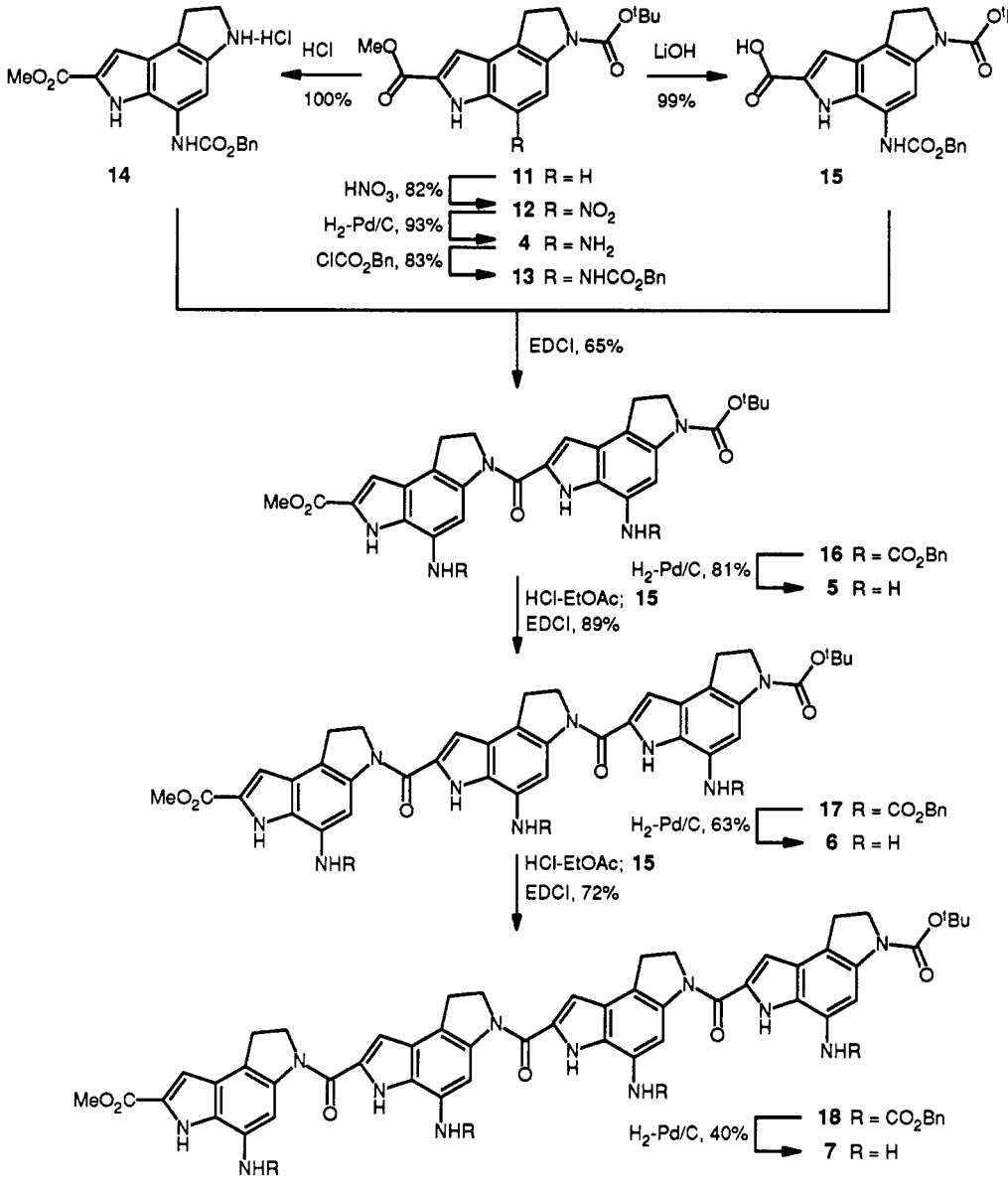

face of the agents. In addition, studies of TACDPI$_n$ (8–10, n = 1–3) establish a significant enhancement of the noncovalent minor groove binding affinity through introduction of an electropositive substituent and stabilizing electrostatic interactions.

Synthesis of ACDPI$_n$ and TACDPI$_n$. The repeating monomer units of agents employed in the study were prepared through functionalization of the readily accessible N^3-*tert*-butyloxycarbonyl derivative of CDPI$_1$ (11) which in turn has been prepared in five steps (55% overall yield)[10] from available materials. Low-temperature nitration of 11 cleanly afforded 12 (82%). Subsequent reduction of the nitro group provided the N^3-*tert*-butyloxycarbonyl derivative of ACDPI$_1$ (4, 77–93%) and protection of the free amine as its benzyloxycarbonyl derivative provided 13 (83%), Scheme I. Lithium hydroxide hydrolysis of the methyl ester of 13 conducted under an inert atmosphere in the presence of sodium dithionite provided 15 (99%). Acid-catalyzed removal of the N^3-*tert*-butyloxycarbonyl group of 13 provided 14 as an unstable salt which was coupled directly with 15 through use of the water-soluble 1-[3-(dimethylamino)propyl]-3-ethylcarbodiimide (EDCI) to provide 16 (65%). The coupling reaction and those to follow were run necessarily as suspensions in dimethylformamide for extended reaction times (48–60 h). The subsequent removal of reagent-derived materials from the coupling product was effectively accomplished by aqueous acid trituration of the insoluble reaction product followed by an organic solvent trituration, and final purification was accomplished by column chromatography. Catalytic hydrogenolysis of 16 removed the two benzyloxycarbonyl groups and provided ACDPI$_2$ (5, 81%). Acid-catalyzed removal of the *tert*-butyloxycarbonyl group of 16 followed by immediate EDCI-promoted coupling of the resulting unstable hydrochloride salt with 15 provided 17 (89%), and subsequent catalytic hydrogenolysis provided ACDPI$_3$ (6, 63%). The agents became increasingly less soluble in organic solvents as their size increased. This proved especially true of the free amines 6 and 7, and the modest conversions in the final hydrogenolysis reactions reflect the difficulty in the chromatographic purification of the agents and not an

(19) Boger, D. L.; Ishizaki, T.; Kitos, P. A.; Suntornwat, O. *J. Org. Chem.* **1990**, *55*, 5823. Boger, D. L.; Ishizaki, T.; Wysocki, R. J., Jr.; Munk, S. A.; Kitos, P. A.; Suntornwat, O. *J. Am. Chem. Soc.* **1989**, *111*, 6461.

(20) Boger, D. L.; Wysocki, R. J., Jr.; Ishizaki, T. *J. Am. Chem. Soc.* **1990**, *112*, 5230.

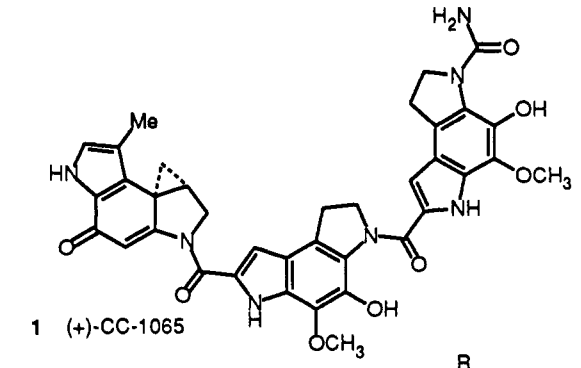

1 (+)-CC-1065

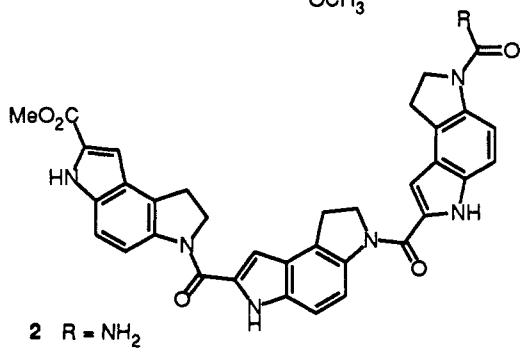

2 R = NH_2
3 R = O^{t}Bu

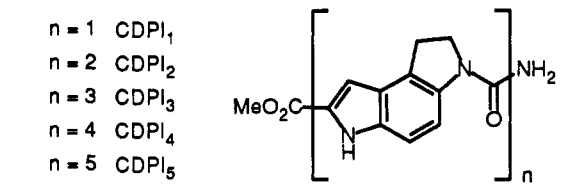

n = 1 $CDPI_1$
n = 2 $CDPI_2$
n = 3 $CDPI_3$
n = 4 $CDPI_4$
n = 5 $CDPI_5$

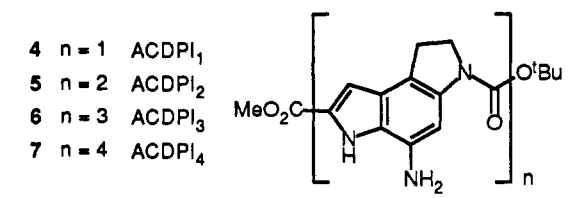

4 n = 1 $ACDPI_1$
5 n = 2 $ACDPI_2$
6 n = 3 $ACDPI_3$
7 n = 4 $ACDPI_4$

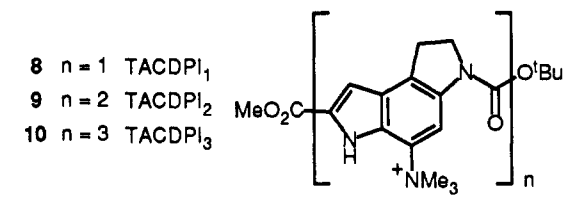

8 n = 1 $TACDPI_1$
9 n = 2 $TACDPI_2$
10 n = 3 $TACDPI_3$

Figure 1.

inherent problem in the deprotection reaction. In a similar fashion, acid-catalyzed deprotection of **17** followed by EDCI-promoted coupling of the resultant hydrochloride salt with **15** provided **18** (72%). Subjection of **18** to the conditions of catalytic hydrogenolysis provided $ACDPI_4$ (**7**, 40%).

The final series of agents, $TACDPI_n$ (**8–10**), was prepared through exhaustive methylation of the free amines **4–6**, eq 1. The resulting agents became increasingly more water soluble and less organic soluble as the size of the agent and number of quaternary amines increased. For $TACDPI_3$ and $TACDPI_2$, this precluded isolation by standard chromatographic methods and required that the final purification be conducted by recrystallization for which no deliberate effort was made to ensure full recovery of the desired agent. Consequently, the conversions reported for the preparation of **9** and **10** exceed that detailed for their isolation. The trimer agent, $TACDPI_3$ (**10**), proved particularly difficult to crystallize and was found to be optimally conducted with the methanesulfonate salt derived from exhaustive methylation with dimethylsulfate.

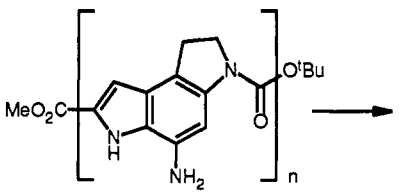

4 n = 1 $ACDPI_1$ (MeI)
5 n = 2 $ACDPI_2$ (MeI)
6 n = 3 $ACDPI_3$ (Me_2SO_4)

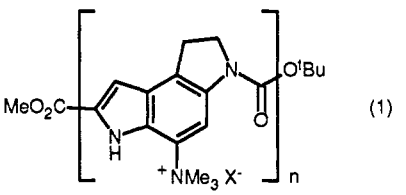

(1)

8 n = 1 $TACDPI_1$ X = I
9 n = 2 $TACDPI_2$ X = I
10 n = 3 $TACDPI_3$ X = $MeSO_4$

DNA Binding Studies. The relative and absolute binding constants of the agents were determined by fluorescence measurements of the displacement of prebound ethidium bromide from DNA.[9,21] Under the conditions employed, the agents do not interfere with the measurement of the characteristic fluorescence loss due to the displacement of DNA-bound ethidium bromide. In contrast to prior agents studied using this technique, the binding of $CDPI_3$ to poly[dA]-poly[dT] and poly[d(A-T)]-poly[d(A-T)] follows an ideal model for agent noncompetitive binding.[22] This first was evident in studies[9] with $CDPI_3$ (**2**, r = 0.2) and PDE-I_2 (r = 0.27) upon examination of the linear plots of percent fluorescence versus r, $[agent]_T/[base\text{-}pair]_T$ where $[agent]_T$ and $[base\text{-}pair]_T$ constitute the total agent concentration and the total base-pair concentration employed in the assay. The X-intercept of the linear plots was found to correspond to the ideal [agent]/[base-pair] ratios of 0.2 and 0.27, respectively. This is illustrated with the *tert*-butyloxycarbonyl derivative of $CDPI_3$ (**3**) examined in the present study (Figure 2). This corresponds to an agent/base-pair ratio of 1/5 for $CDPI_3$ and nicely accommodates the expected minor groove binding which spans five base-pairs. Consequently, the noncompetitive binding of $CDPI_3$ proceeds with the linear displacement of prebound ethidium bromide in a manner that permits the accurate quantification of the DNA-bound agent and the accurate measurement of absolute binding constants according to eq 2 at 50% fluorescence.[9]

$$K = \frac{1}{[agent]_T - 0.5[base\text{-}pair]_T r} \qquad (2)$$

r = agent/base-pair binding site size

The plots of percent fluorescence versus r for the agents in the present study proved linear, and the X-intercepts

(21) Morgan, A. R.; Lee, J. S.; Pulleyblank, D. E.; Murray, N. L.; Evans, D. H. *Nucl. Acids Res.* **1979**, *7*, 547.
(22) Baguley, B. C.; Denny, A. W.; Atwell, G. J.; Cain, B. F. *J. Med. Chem.* **1981**, *24*, 170.

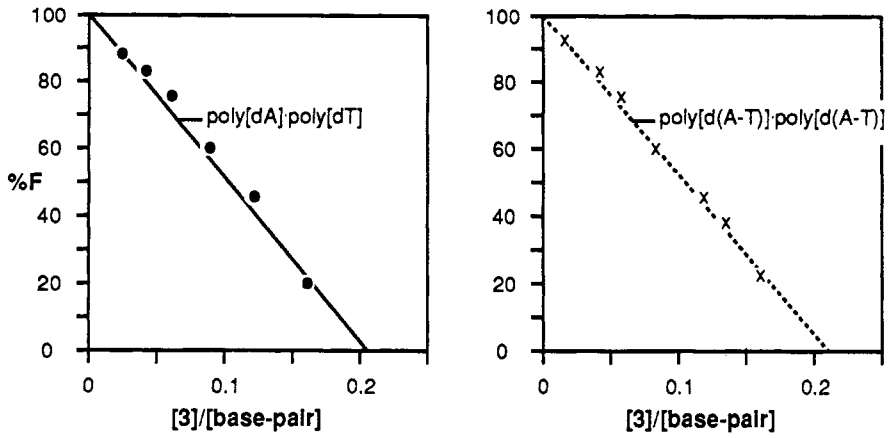

Figure 2. Percent fluorescence versus [3]/[base-pair].

Table I. Binding Constants and Estimated Free Energies of Binding[a]

agent	K_b (M^{-1})	$\Delta G°$ (kcal/mol, 298 K)	agent	K_b (M^{-1})	$\Delta G°$ (kcal/mol, 298 K)	agent[b]	K_b (M^{-1})	$\Delta G°$ (kcal/mol, 298 K)
				Poly[dA]-Poly[dT]				
$CDPI_1$	6.4×10^4	−6.6	$ACDPI_1$	5.7×10^3	−5.1	$TACDPI_1$	3.8×10^5	−7.6
$CDPI_2$	3.2×10^5	−7.5	$ACDPI_2$	2.8×10^4	−6.1	$TACDPI_2$	1.4×10^7	−9.8
$CDPI_3$	1.8×10^7	−9.9	$ACDPI_3$	9.6×10^5	−8.2	$TACDPI_3$	1.3×10^8	−11.1
$CDPI_4$	1.4×10^6	−8.4	$ACDPI_4$	5.6×10^5	−7.8			
$CDPI_5$	2.1×10^6	−8.6						
3	1.5×10^7	−9.8						
				Poly[d(A-T)]-Poly[d(A-T)]				
$CDPI_1$	6.1×10^4	−6.5	$ACDPI_1$	4.3×10^3	−5.0	$TACDPI_1$	4.5×10^5	−7.7
$CDPI_2$	9.6×10^4	−6.8	$ACDPI_2$	2.1×10^4	−5.9	$TACDPI_2$	2.1×10^7	−10.0
$CDPI_3$	8.9×10^6	−9.5	$ACDPI_3$	1.4×10^6	−8.4	$TACDPI_3$	5.4×10^8	−11.9
$CDPI_4$	6.7×10^5	−8.0	$ACDPI_4$	2.2×10^5	−7.3			
$CDPI_5$	6.7×10^5	−8.0						
3	7.3×10^6	−9.3						
				Poly[dG]-Poly[dC]				
$CDPI_1$	5.1×10^4	−6.4	$ACDPI_1$	3.2×10^3	−4.8	$TACDPI_1$	2.1×10^4	−5.9
$CDPI_2$	6.9×10^4	−6.6	$ACDPI_2$	4.3×10^3	−5.0	$TACDPI_2$	1.0×10^6	−8.2
$CDPI_3$	2.0×10^5	−7.2	$ACDPI_3$	1.4×10^5	−7.0	$TACDPI_3$	1.6×10^6	−8.4
$CDPI_4$	4.1×10^5	−7.7	$ACDPI_4$	1.0×10^5	−6.8			
$CDPI_5$	4.9×10^5	−7.8						
3	2.1×10^5	−7.3						

[a] Unless indicated otherwise, $r = 0.6$, 0.3, 0.2, and 0.25 for $n = 1$, 2, 3, and 4 or 5, respectively. [b] For $TACDPI_2$, $r = 0.23$; for $TACDPI_3$, $r = 0.11$ as determined from the X-intercept of plots of percent fluorescence vs r.

were employed to determine the characteristic r value which, in general, corresponded to the expected ideal value. The results of the DNA binding studies are presented in Table I, and the binding constants were calculated using the noncompetitive binding model[9] with r values of 0.6, 0.3, 0.2, and 0.25 for the agent monomer, dimer, trimer, and tetramer, respectively, unless otherwise indicated. In initial studies and for comparison purposes, the absolute binding constants for $CDPI_3$ were calculated using a conventional competitive binding model[22] and did not differ significantly from those calculated using the noncompetitive binding model.[9]

$ACDPI_n$. Consistent with past observations with $CDPI_n$[9] (Figure 3A), the $ACDPI_3$ binding constant for poly[dA]-poly[dT] proved largest within the $ACDPI_n$ series of agents studied, and this is apparent from the plot of log K_b versus agent, Figure 3B: $ACDPI_4 < ACDPI_3 > ACDPI_2 > ACDPI_1$. As discussed in detail elsewhere for the $CDPI_n$ oligomers, we have interpreted the unexpected behavior of the higher oligomer agents to represent kinetic binding within the minor groove in partial-bound forms, i.e. $ACDPI_2$-bound or $ACDPI_3$-bound $ACDPI_4$.[9] This may be attributed to at least two features of the agents. As the size of the oligomeric agents surpass the trimer, a large number of accessible conformations are available to the agent in addition to the helical conformation required for full agent binding. This becomes more pronounced as the size of the agent increases and represents a barrier to achieving full structure binding. Perhaps more importantly, the trimer binding covers five base-pairs constituting half of a full B-DNA helix turn. For a relatively rigid agent such as $ACDPI_n$ or $CDPI_n$, this represents the largest accessible minor groove DNA binding site that permits both ends of the agent to achieve near synchronous binding through a helical conformation. For larger agents including $ACDPI_4$ and $CDPI_4$, both ends of the agent may not bind synchronously since the binding termini lie on opposite faces of the helix. Moreover, the relatively rigid structure of the agents, the depth to which the agents penetrate into the minor groove, and its narrow width require that the agents undergo decomplexation and rebinding or that the DNA undergo substantial local unwinding in order to permit the conformational interconversion between partial and full bound agents. In the prior studies with $CDPI_n$,[9] we established through thermal denaturization studies that prolonged incubation of the tetramer agent with DNA (10 d versus 30 min) did lead to a complex that was more stable than the initial kinetic complex, that the slow interconversion of the two distinct complexes could be followed over the prolonged incubation, and that the latter

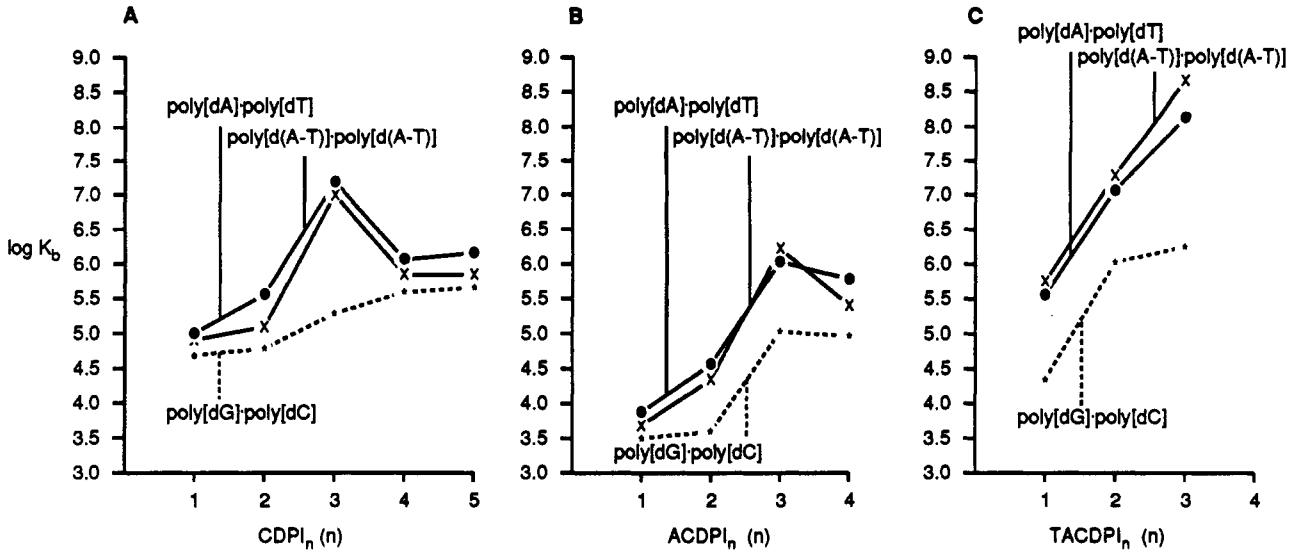

Figure 3.

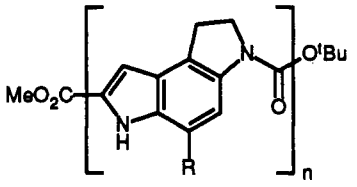

- Affinity
  - n = 3 > 4, 5 > 2 > 1
  - R = $^+NMe_3$ > H > NH_2
- Specificity
  - AT > GC for n = 3
  - $\Delta\Delta G^\circ$ = 1.2 - 2.7 kcal

poly[dA]·poly[dT]

ΔG° (298°K, kcal/mol)

R	n = 1	2	3	4	5
NH_2	-5.1	-6.1	-8.2	-7.8	
H	-6.6	-7.5	-9.9	-8.4	-8.6
$^+NMe_3$	-7.6	-9.8	-11.1		

n = 3 ΔG° (298°K, kcal/mol)

R	poly[dA]-poly[dT]	poly[dG]-poly[dC]	$\Delta\Delta G^\circ$
NH_2	-8.2	-7.0	-1.2
H	-9.9	-7.2	-2.7
$^+NMe_3$	-11.1	-8.4	-2.7

Figure 4.

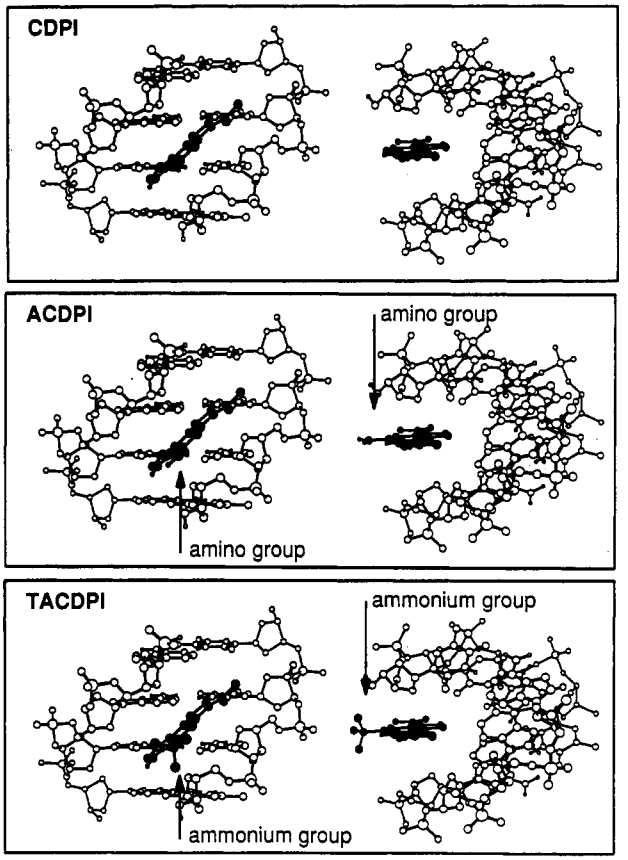

Figure 5. Two views of $d(A)_{2-5}$-$d(T)_{2-5}$:CDPI, $d(A)_{2-5}$-$d(T)_{2-5}$:ACDPI, and $d(A)_{2-5}$-$d(T)_{2-5}$:TACDPI taken from $d(A)_{10}$-$d(T)_{10}$:$CDPI_3$, $d(A)_{10}$-$d(T)_{10}$:$ACDPI_3$, and $d(A)_{10}$-$d(T)_{10}$:$TACDPI_3$ models (MacroModel, AMBER force field supplemented with agent parameters).

complex was more stable than that derived from the corresponding trimer agent. We assume that $ACDPI_4$ is behaving in a comparable manner, see Figure 3, parts A and B. Consistent with the prior observations made with $CDPI_n$, the experimental results indicated that $ACDPI_3$ is the most effective binding agent within the $ACDPI_n$ series and possesses the optimal combination of size and structural features that facilitate kinetically rapid and thermodynamically stable minor groove binding.

Identical trends and nearly identical binding constants for $ACDPI_n$ were observed with poly[d(A-T)]-poly[d(A-T)]. In marked contrast, the binding of $ACDPI_n$ with poly-[dG]-poly[dC] was substantially reduced, although a similar trend in binding affinity was observed: $ACDPI_4$ < $ACDPI_3$ > $ACDPI_2$ > $ACDPI_1$.

Perhaps more important is the comparison of the $ACDPI_n$ versus $CDPI_n$ agents. The introduction of an amino group onto the outer face of $CDPI_n$ resulted in a substantial reduction in the agent DNA minor groove binding affinity, Figure 4, without altering the inherent AT binding selectivity. This may be attributed in part to the strategic placement of the amino group on the outer face of the DNA–agent complex between the walls of the

minor groove and proximal to phosphates in the DNA backbone, cf. Figure 5. At a pH of 8 as employed in the assay, the $ACDPI_n$ agents possess a free amine resulting in an apparent and substantial destabilizing electrostatic interaction with the negatively charged phosphate backbone of DNA.

TACDPI$_n$. Having established that the introduction of an electronegative substituent onto the peripheral face of $CDPI_n$ diminished its DNA binding affinity, a complementary class of agents bearing an electropositive C-5 substituent was examined. The study of the series of $TACDPI_n$ agents in which the C-5 primary amine of $ACDPI_n$ was converted to a quaternary amine through exhaustive methylation proved revealing. Consistent with expectations, the noncovalent binding affinity of the agents increased as the size of the agent was increased, $TACDPI_3$ > $TACDPI_2$ > $TACDPI_1$. Similar to the trends observed with $CDPI_n$ and $ACDPI_n$, $TACDPI_n$ exhibited a substantial binding preference for AT-rich versus GC-rich DNA, and this preference was most evident with the trimer, Figure 3C (n = 3, $\Delta\Delta G°$ = −2.7 to −3.5 kcal). In addition, the relative binding affinity of the agents substantially exceeded that of $ACDPI_n$ and significantly surpassed that of the parent $CDPI_n$ agents. We attribute this increased DNA binding affinity to the stabilizing electrostatic interaction between the negatively charged phosphates in the DNA backbone and the strategically placed, positively charged ammonium group on the peripheral face of agent, Figure 5. Importantly, this increased binding affinity derived from stabilizing electrostatic interactions is of such a magnitude that it overrides the effect of the increased water solubility of the agents that would be expected to diminish the inherent hydrophobic binding affinity.

Role of the Terminal Urethane. Finally, the relative and absolute binding of the two $CDPI_n$ agents, **2** versus **3**, proved indistinguishable within the experimental error inherent in the measurements for each of the three DNAs examined indicating that the terminal urethane of **2**, like that found in (+)-CC-1065, is not contributing to the affinity or specificity of the DNA minor groove binding.

Conclusions. Comparable to observations made with $CDPI_n$,[9] examination of the $ACDPI_n$ oligomers revealed that $ACDPI_3$ is the optimal DNA minor groove binding agent in the series, that the tetramer and higher oligomers exhibit DNA binding properties intermediate between those of the corresponding dimer and trimer, and that the agents exhibit a selectivity for AT-rich versus GC-rich DNA which is most pronounced with $ACDPI_3$. Similarly, the examination of the $TACDPI_n$ oligomers revealed a pronounced AT-rich versus GC-rich binding selectivity. The direct comparison of $CDPI_n$ with $ACDPI_n$ revealed that the introduction of a C-5 amino substituent onto the peripheral face of the agent resulted in a substantial reduction in the DNA minor groove binding affinity that we attribute to the introduction of destabilizing electrostatic interactions. In contrast, the comparison of $CDPI_n$ with $TACDPI_n$ revealed that the introduction of a C-5 quaternary amine resulted in a substantial enhancement in the DNA binding affinity attributable to the introduction of stabilizing electrostatic interactions.[23]

Experimental Section

Methyl 3-(*tert*-Butyloxycarbonyl)-5-nitro-1,2-dihydro-3*H*-pyrrolo[3,2-*e*]indole-7-carboxylate (12). A solution of 11[10] (600 mg, 1.9 mmol) in dry nitromethane (10 mL) was treated with concentrated HNO_3 (0.20 mL, 3.1 mmol, 1.6 equiv) at 0 °C (15 min). Additional HNO_3 (0.05 mL, 0.78 mmol, 0.4 equiv) was added, and the mixture was stirred for 1.5 h at 0 °C. The mixture was poured into water (20 mL) and extracted with CH_2Cl_2 (4 × 15 mL). The combined organic phase was dried (Na_2SO_4) and concentrated in vacuo. Chromatography (2 cm × 13 cm, gradient elution with 0–10% EtOAc–hexane) afforded **12** (562 mg, 685 mg theoretical, 82%) as an orange-yellow crystalline solid: mp 198–200.5 °C (orange needles, hexane–EtOAc); ^1H NMR ($CDCl_3$, 300 MHz) δ 10.30 (br s, 1 H, NH), 8.95 (br s, 1 H, C4-H), 7.20 (d, 1 H, J = 1 Hz, C8-H), 4.20 (t, 2 H, J = 8.5 Hz, $ArCH_2CH_2NR$), 4.02 (s, 3 H, CO_2CH_3), 3.40 (t, 2 H, J = 8.5 Hz, $ArCH_2CH_2NR$), 1.62 (br s, 9 H, *t*Bu); ^{13}C NMR ($CDCl_3$, 75 MHz) δ 160.7, 151.9, 136.7, 132.9, 131.4, 130.1, 126.9, 126.2, 110.0, 109.0, 106.3, 52.3, 47.7, 28.2, 26.5; IR (KBr) ν_{max} 3463, 2975, 1701, 1654, 1636, 1588, 1540 cm^{-1}; EIMS m/e (relative intensity) 361 (M^+, 4), 305 (49), 261 (16), 229 (19), 57 (base); CIMS (isobutane) m/e (relative intensity) 362 (M^+ + H, base); EIHRMS m/e 361.1269 ($C_{17}H_{19}N_3O_6$ requires 361.1274).

Anal. Calcd for $C_{17}H_{19}N_3O_6$: C, 56.51; H, 5.30; N, 11.63. Found: C, 56.42; H, 5.43; N, 11.43.

A minor side product, methyl 3-(*tert*-butyloxycarbonyl)-8-nitro-1,2-dihydro-3*H*-pyrrolo[3,2-*e*]indole-7-carboxylate was isolated in less than 10% yield: mp 216–218 °C dec (yellow fluffy solid, hexane–EtOAc); ^1H NMR (DMSO-d_6, 300 MHz) δ 13.16 (br s, 1 H, NH), 7.94 (br s, 1 H, C4-H), 7.32 (d, 1 H, J = 9 Hz, C5-H), 3.92 (t, 2 H, J = 8 Hz, $ArCH_2CH_2NR$), 3.93 (s, 3 H, CO_2CH_3), 3.31 (t, 2 H, J = 8 Hz, $ArCH_2CH_2NR$), 1.49 (s, 9 H, *t*Bu); ^{13}C NMR (DMSO-d_6, 75 MHz) δ 160.2, 152.0, 140.0, 131.0, 128.0, 127.3, 121.0, 117.2, 114.5, 112.5, 80.1, 53.0, 47.6, 28.0, 27.0; IR (KBr) ν_{max} 3432, 2974, 1692, 1522, 1506 cm^{-1}.

Methyl 5-Amino-3-(*tert*-butyloxycarbonyl)-1,2-dihydro-3*H*-pyrrolo[3,2-*e*]indole-7-carboxylate (4). A solution of **12** (690 mg, 1.96 mmol) in dry THF (20 mL) was treated with 10% Pd–C (1.7 g, 0.25 wt equiv) and placed under 1 atm of H_2 (12 h). The catalyst was removed by filtration through Celite, and the solvent was removed in vacuo. Chromatography (after dry packing with 20 g of SiO_2, 2 cm × 18 cm, gradient elution with 5–22% EtOAc–hexane) afforded $ACDPI_1$ (**4**, 500 mg, 649 mg theoretical, 77%; typically 93–77%) as pale green solid: mp 215 °C dec (light green plates, EtOAc–hexane); ^1H NMR (DMSO-d_6, 300 MHz) δ 11.45 (br s, 1 H, NH), 7.20 (br s, 1 H, C4-H), 6.90 (d, 1 H, J = 1 Hz, C8-H), 5.44 (br s, 2 H, NH_2), 3.94 (t, 2 H, J = 8.5 Hz, $ArCH_2CH_2NR$), 3.88 (s, 3 H, CO_2CH_3), 3.08 (t, 2 H, J = 8.5 Hz, $ArCH_2CH_2NR$), 1.51 (br s, 9 H, *t*Bu); ^{13}C NMR (DMSO-d_6, 75 MHz) δ 162.5, 152.5, 137.5, 134.0, 127.0, 125.2, 124.8, 108.5, 106.2, 97.2, 79.8, 52.2, 48.5, 28.6, 26.0; IR (KBr) ν_{max} 3443, 3370, 3327, 2977, 2933, 1689, 1597, 1531, 1516 cm^{-1}; EIMS m/e (relative intensity) 331 (M^+, 20), 243 (base), 198 (18), 171 (16), 143 (12), 57 (67); CIMS (isobutane) m/e 332 (M^+ + H, base); EIHRMS m/e 331.1525 ($C_{17}H_{21}O_4N_3$ requires 331.1532).

Anal. Calcd for $C_{17}H_{21}N_3O_4$: C, 61.62; H, 6.30; N, 12.68. Found: C, 61.62; H, 6.65; N, 12.84.

Methyl 5-[(Benzyloxycarbonyl)amino]-3-(*tert*-butyloxycarbonyl)-1,2-dihydro-3*H*-pyrrolo[3,2-*e*]indole-7-carboxylate (13). A solution of **4** (332 mg, 1.0 mmol) in THF (5 mL) at 0 °C was treated sequentially with K_2CO_3 (279 mg, 2.02 mmol, 2.0 equiv) and benzyl chloroformate (0.16 mL, 1.11 mmol, 1.1 equiv) and stirred vigorously at 0 °C for 3 h. Additional benzyl chloroformate (0.13 mL, 0.91 mmol, 0.9 equiv) was added, and the mixture was stirred at 0 °C (1 h) and 23 °C (1 h). The reaction mixture was diluted with H_2O (50 mL) and extracted with CH_2Cl_2 (3 × 50 mL). The combined organic phase was dried (Na_2SO_4) and concentrated in vacuo. Chromatography (2 cm × 16 cm, gradient elution with 0–18% EtOAc–hexane) provided **13** (389 mg, 461 mg theoretical, 83%) as a white fluffy solid: mp 185–186.5 °C (fine white needles, EtOAc–hexane); ^1H NMR ($CDCl_3$, 300 MHz) δ 10.22 (br s, 1 H, NH), 7.75 (br s, 1 H, C4-H), 7.38–7.34 (m, 5 H, PhH), 7.03 (d, 1 H, J = 1 Hz, C8-H), 5.24 (s, 2 H, $PhCH_2$), 4.07 (t, 2 H, J = 8.5 Hz, $ArCH_2CH_2NR$), 3.92 (s, 3 H, CO_2CH_3), 3.21 (t, 2 H, J = 8.5 Hz, $ArCH_2CH_2NR$), 1.55 (br s, 9 H, *t*Bu); IR (KBr) ν_{max} 3314, 3154, 2976, 1712, 1697, 1686, 1636, 1609, 1550, 1510 cm^{-1}; EIMS m/e (relative intensity) 465 (M^+, 4), 409 (20), 274 (30), 91 (base); CIMS (isobutane) m/e 466 (M^+ + H, base); EIHRMS m/e 465.1888 ($C_{25}H_{27}N_3O_6$ requires 465.1900).

(23) In vitro cytotoxic activity for the agents (IC_{50}, μg/mL, L1210): $CDPI_1$ (>50), $CDPI_2$ (>50), $CDPI_3$ (0.6), $CDPI_4$ (0.007), $CDPI_5$ (>20), $ACDPI_1$ (>1), $ACDPI_2$ (>1), $ACDPI_3$ (>1), $TACDPI_1$ (>50), $TACDPI_2$ (>50), $TACDPI_3$ (>50).

Anal. Calcd for $C_{25}H_{27}N_3O_6$: C, 64.51; H, 5.85; N, 9.03. Found: C, 64.54; H, 6.18; N, 9.21.

5-[(Benzyloxycarbonyl)amino]-3-(*tert*-butyloxycarbonyl)-1,2-dihydro-3*H*-pyrrolo[3,2-*e*]indole-7-carboxylic Acid (15). A solution of **13** (81.6 mg, 0.82 mmol) in THF–H_2O (3:1, 3 mL) under argon was treated with LiOH–H_2O (172 mg, 4.10 mmol, 5.0 equiv) and sodium dithionite (285 mg, 1.64 mmol, 2.0 equiv) and stirred at 23 °C (72 h). The reaction mixture was poured into H_2O (15 mL), acidified to pH 4 with the addition of 10% aqueous HCl, and extracted with EtOAc (4 × 25 mL). The combined organic layer was washed with saturated aqueous NaCl (15 mL), dried (Na_2SO_4), and concentrated in vacuo. The crude product was slurried with silica gel (550 mg) in CH_2Cl_2, the solvent was removed in vacuo, and the dry silica gel was loaded onto a flash chromatography column. Chromatography (2 cm × 9 cm, gradient elution with 50–100% EtOAc–hexane then 10% MeOH–EtOAc) provided **15** (367 mg, 370 mg theoretical, 99%) as a light green solid: mp 205–207 °C dec (greenish white flakes, EtOAc); ^{1}H NMR (DMSO-d_6, 300 MHz) δ 11.55 (s, 1 H, NH), 9.60 (s, 1 H, CONH), 8.48 (br s, 1 H, C4-H), 7.49–7.31 (m, 5 H, PhH), 6.94 (d, 1 H, J = 1.5 Hz, C8-H), 5.20 (s, 2 H, $PhCH_2$), 3.99 (t, 2 H, J = 8.4 Hz, C1-H_2), 3.15 (t, 2 H, J = 8.4 Hz, C2-H_2), 1.52 (br s, 9 H, *t*Bu); IR (KBr) ν_{max} 3348, 2976, 1696, 1548 cm^{-1}; EIMS m/e (relative intensity) 451 (M^+, 2), 108 (45), 91 (34), 56 (base); CIMS (isobutane) m/e 452 (M^+ + H, base); EIHRMS m/e 451.1752 ($C_{24}H_{25}N_3O_6$ requires 451.1743).

Methyl 5-[(Benzyloxycarbonyl)amino]-3-[[5′-[(benzyloxycarbonyl)amino]-3′-(*tert*-butyloxycarbonyl)-1′,2′-dihydro-3′*H*-pyrrolo[3′,2′-*e*]indol-7′-yl]carbonyl]-1,2-dihydro-3*H*-pyrrolo[3,2-*e*]indole-7-carboxylate (16). The agent **13** (219 mg, 0.47 mmol) was treated with a solution of 3 M HCl in EtOAc (5 mL), and the mixture was stirred under argon at 23 °C (1 h). Removal of the solvent in vacuo provided the crude unstable hydrochloride salt **14** as a gray solid in quantitative yield.

A solution of **14** (143 mg, 0.36 mmol), **15** (179 mg, 0.40 mmol, 1.2 equiv), EDCI (224 mg, 1.17 mmol, 3.3 equiv), and $NaHCO_3$ (262 mg, 3.12 mmol, 8.7 equiv) in dry DMF (3.0 mL) was stirred vigorously under nitrogen at 23 °C (49 h). The reaction mixture was poured into H_2O (25 mL) and acidified to pH 4–5 with the addition of 10% aqueous HCl. The mixture was extracted with EtOAc (4 × 100 mL), and the combined organic layer was washed with saturated aqueous NaCl (30 mL), dried (Na_2SO_4), and concentrated in vacuo. Chromatography (2 cm × 19 cm, gradient elution with 0–40% EtOAc–hexane) gave **16** (187 mg, 287 mg theoretical, 65%) as a pale white solid: mp 228–229.5 °C dec (fine white flakes, CH_2Cl_2–hexane); ^{1}H NMR (DMSO-d_6, 300 MHz) δ 11.74 (br s, 1 H, NH), 11.64 (br s, 1 H, NH), 9.77 (br s, 1 H, CONH), 9.64 (br s, 1 H, CONH), 9.00 (br s, 1 H, C4-H), 8.45 (very br s, 1 H, C4′-H), 7.50–7.36 (m, 10 H, PhH), 7.11 (d, 1 H, J = 1.6 Hz, C8′-H), 6.97 (d, 1 H, J = 1.6 Hz, C8-H), 5.21 (s, 4 H, $PhCH_2$), 4.60 (t, 2 H, J = 7.9 Hz, C2-H_2), 3.99 (t, 2 H, J = 7.9 Hz, C2′-H_2), 3.88 (s, 3 H, CO_2CH_3), 3.37 (t, 2 H, J = 7.9 Hz, C1-H_2), 3.18 (t, 2 H, J = 7.9 Hz, C1′-H_2), 1.54 (s, 9 H, *t*Bu); IR (KBr) ν_{max} 3424, 1702, 1528, 1388, 1244, 1138, 736 cm^{-1}; FABMS (*m*-nitrobenzyl alcohol) m/e 799 (M^+ + H); FABHRMS (*m*-nitrobenzyl alcohol) m/e 799.2877 ($C_{44}H_{42}N_6O_9$ + H^+ requires 799.3091).

Anal. Calcd for $C_{44}H_{42}N_6O_9$: C, 66.16; H, 5.30; N, 10.52. Found: C, 65.08; H, 4.97; N, 10.55.

Methyl 5-[(Benzyloxycarbonyl)amino]-3-[[5′-[(benzyloxycarbonyl)amino]-3′-[[5″-[(benzyloxycarbonyl)amino]-3″-(*tert*-butyloxycarbonyl)-1″,2″-dihydro-3″*H*-pyrrolo[3″,2″-*e*]indol-7″-yl]carbonyl]-1′,2′-dihydro-3′*H*-pyrrolo[3′,2′-*e*]indol-7′-yl]carbonyl]-1,2-dihydro-3*H*-pyrrolo[3,2-*e*]indole-7-carboxylate (17). A solution of **16** (50.4 mg, 0.063 mmol) in 3 M HCl in EtOAc (1 mL) was stirred under N_2 for 30 min. Removal of the solvent in vacuo afforded the crude hydrochloride salt as a green solid.

The crude salt (0.063 mmol), **15** (34 mg, 0.075 mmol, 1.2 equiv), EDCI (36 mg, 0.19 mmol, 3.0 equiv), and $NaHCO_3$ (42 mg, 0.50 mmol, 8.0 equiv) in dry DMF (1.5 mL) under N_2 were stirred at 23 °C (48 h). The reaction mixture was poured into H_2O (25 mL), acidified to pH 4 with the addition of 10% aqueous HCl, and extracted with EtOAc (4 × 35 mL). The organic layer was washed with saturated aqueous NaCl (20 mL), dried (Na_2SO_4), and concentrated in vacuo. Chromatography (2 cm × 9 cm, 20–100% EtOAc–hexane gradient elution) provided **17** (63.3 mg, 70.9 mg theoretical, 89%) as a pale white solid: mp > 275 °C dec (fine white flakes, EtOAc); ^{1}H NMR (DMSO-d_6, 300 MHz) δ 11.77 (br s, 1 H, NH), 11.73 (br s, 1 H, NH), 11.65 (br s, 1 H, NH), 9.81 (br s, 1 H, CONH), 9.77 (br s, 1 H, CONH), 9.64 (br s, 1 H, CONH), 9.00 (br s, 1 H, C4-H), 8.96 (br s, 1 H, C4′-H), 8.45 (very br s, 1 H, C4″-H), 7.49–7.32 (m, 15 H, PhH), 7.14 (s, 1 H, C8″-H or C8′-H), 7.12 (s, 1 H, C8′-H or C8″-H), 7.02 (s, 1 H, C8-H), 5.20 (s, 6 H, $PhCH_2$), 4.64 (t, 4 H, J = 7.6 Hz, C2-H_2 and C2′-H_2), 4.03 (t, 2 H, J = 7.6 Hz, C2″-H_2), 3.87 (s, 3 H, CO_2CH_3), 3.40 (m, 4 H, C1-H_2 and C1′-H_2), 3.23 (t, 2 H, J = 6.2 Hz, C1″-H_2), 1.52 (br s, 9 H, *t*Bu); IR (KBr) ν_{max} 3426, 2934, 1700, 1636, 1524 cm^{-1}; FABMS (DTT/DTE) m/e 1132 (M^+ + H).

Anal. Calcd for $C_{63}H_{57}N_9O_{12}$: C, 66.83; H, 5.07; N, 11.13. Found: C, 66.47; H, 5.28; N, 11.47.

Methyl 5-[(Benzyloxycarbonyl)amino]-3-[[5′-[(benzyloxycarbonyl)amino]-3′-[[5″-[(benzyloxycarbonyl)amino]-3″-[[5‴-[(benzyloxycarbonyl)amino]-3‴-(*tert*-butyloxycarbonyl)-1‴,2‴-dihydro-3‴*H*-pyrrolo[3‴,2‴-*e*]indol-7‴-yl]carbonyl]-1″,2″-dihydro-3″*H*-pyrrolo[3″,2″-*e*]indol-7″-yl]carbonyl]-1′,2′-dihydro-3′*H*-pyrrolo[3′,2′-*e*]indol-7′-yl]carbonyl]-1,2-dihydro-3*H*-pyrrolo[3,2-*e*]indole-7-carboxylate (18). A solution of **17** (50.8 mg, 0.045 mmol) in 3 M HCl in EtOAc (2 mL) under N_2 was stirred at 23 °C (45 min). Removal of solvent in vacuo provided the crude unstable hydrochloride salt (48 mg, 48 mg theoretical, 100%) as a dark green solid.

The crude hydrochloride salt (0.045 mmol), **15** (20.3 mg, 0.048 mmol, 1.1 equiv), EDCI (26 mg, 0.14 mmol, 3.0 equiv), and $NaHCO_3$ (30.2 mg, 0.36 mmol, 8.0 equiv) in dry DMF (1.5 mL) under N_2 were stirred vigorously at 23 °C (60 h). The reaction mixture was poured into H_2O (5 mL) and acidified to pH 4 with the addition of 10% aqueous HCl. The mixture was slurried, and the suspended solid was collected by centrifugation. The solid was washed with H_2O (3 × 5 mL) and EtOAc (2 × 5 mL). The crude product was dry packed onto a flash chromatography column. Chromatography (2 cm × 12 cm, gradient elution with 50–100% EtOAc–hexane and then 5% MeOH–EtOAc) provided **18** (47.3 mg, 65.7 mg theoretical, 72%) as a light brown solid: mp > 275 °C (brown flakes, EtOAc–hexane); ^{1}H NMR (DMSO-d_6, 300 MHz) δ 11.77 (br s, 3 H, NH), 11.66 (br s, 1 H, NH), 9.83 (m, 3 H, CONH), 9.66 (br s, 1 H, CONH), 9.02 (br s, 3 H, C4-H, C4′-H, and C4″-H), 8.03 (very br s, 1 H, C4‴-H), 7.58–7.30 (m, 20 H, PhH), 7.15 (br s, 3 H, C8′-H, C8″-H, C8‴-H), 7.04 (br s, 1 H, C8-H), 5.23 (s, 8 H, $PhCH_2$), 4.70–4.60 (m, 4 H, C2-H_2, C2′-H_2), 4.20 (t, 2 H, J = 7.6 Hz, C2″-H), 4.04 (t, 2 H, J = 7.6 Hz, C2‴-H_2), 3.89 (s, 3 H, CO_2CH_3), 3.48–3.25 (m, 6 H, partially obscured by H_2O, C1-H_2, C1′-H_2, and C1″-H_2), 3.02 (t, 2 H, partially obscured by H_2O, C1‴-H_2), 1.55 (br s, 9 H, *t*Bu); IR (KBr) ν_{max} 3856, 3752, 3320, 2950, 1702, 1622, 1524 cm^{-1}; FABMS (*m*-nitrobenzyl alcohol) m/e 1465 (M^+ + H), 1487 (M^+ + Na).

Methyl 5-Amino-3-[[5′-amino-3′-(*tert*-butyloxycarbonyl)-1′,2′-dihydro-3′*H*-pyrrolo[3′,2′-*e*]indol-7′-yl]carbonyl]-1,2-dihydro-3*H*-pyrrolo[3,2-*e*]indole-7-carboxylate (5). A solution of **16** (121 mg, 0.15 mmol) in dry THF (1.5 mL) under N_2 was treated with 10% palladium on carbon (42 mg, 0.35 wt equiv). The mixture was stirred under a H_2 atmosphere (1 atm) at 23 °C (66 h). The reaction mixture was filtered through Celite to remove the catalyst, and the filtrate was concentrated in vacuo. Chromatography (2 cm × 7.5 cm, 80% EtOAc–hexane, 1% MeOH–EtOAc and 5% MeOH, 15% hexane, 80% EtOAc eluant) provided ACDPI$_2$ (**5**, 64.8 mg, 79.5 mg theoretical, 81%) as a green crystalline solid: mp > 273 °C dec (green plates, CH_2Cl_2); ^{1}H NMR (DMSO-d_6, 300 MHz) δ 11.57 (s, 1 H, NH), 11.22 (s, 1 H, NH), 7.62 (s, 1 H, C4-H), 7.19 (br s, 1 H, C4′-H), 7.01 (s, 1 H, C8′-H), 6.84 (s, 1 H, C8-H), 5.48–5.44 (br d, 4 H, NH_2), 4.55 (t, 2 H, J = 8 Hz, C2-H_2), 3.95 (t, 2 H, J = 8 Hz, C2′-H_2), 3.89 (s, 3 H, CO_2CH_3), 3.21 (t, 2 H, J = 8 Hz, C1-H_2), 3.08 (t, 2 H, J = 8 Hz, C1′-H_2), 1.51 (br s, 9 H, *t*Bu); IR (KBr) ν_{max} 3432, 1686, 1618, 1526, 1426, 1388, 1256, 1138 cm^{-1}; FABMS, (*m*-nitrobenzyl alcohol) m/e 530 (M^+); FABHRMS (*m*-nitrobenzyl alcohol) m/e 531.2316 ($C_{28}H_{30}N_6O_5$ + H^+ requires 531.2355).

Anal. Calcd for $C_{28}H_{30}N_6O_5$: C, 63.38; H, 5.70; N, 15.85. Found: C, 62.97; H, 5.74; N, 15.54.

Methyl 5-Amino-3-[[5′-amino-3′-[[5″-amino-3″-(*tert*-butyloxycarbonyl)-1″,2″-dihydro-3″*H*-pyrrolo[3″,2″-*e*]indol-7″-yl]carbonyl]-1′,2′-dihydro-3′*H*-pyrrolo[3′,2′-*e*]indol-7′-yl]carbonyl]-1,2-dihydro-3*H*-pyrrolo[3,2-*e*]indole-7-

carboxylate (6). A solution of 17 (44.4 mg, 0.039 mmol) in dry THF (2.0 mL) was treated with 10% palladium on carbon (22.2 mg, 0.5 equiv) and placed under an atmosphere of H_2 (1 atm) at 23 °C (43 h). The reaction mixture was filtered through Celite, and the solvent was removed in vacuo. Chromatography (2 cm × 6 cm, 0–20% MeOH–EtOAc gradient elution) afforded $ACDPI_3$ (**6**, 17.9 mg, 28.6 mg theoretical, 63%) as a light green solid: mp > 275 °C dec (green plates, THF); ^1H NMR (DMSO-d_6, 300 MHz) δ 11.57 (br s, 1 H, NH), 11.33 (br s, 1 H, NH), 11.21 (br s, 1 H, NH), 7.63 (br s, 1 H, C4-H), 7.59 (br s, 1 H, C4′-H), 7.20 (br s, 1 H, C4″-H), 7.00 (s, 1 H, C8″-H or C8′-H), 6.95 (s, 1 H, C8′-H or C8″-H), 6.85 (s, 1 H, C8-H), 5.52–5.43 (m, 6 H, NH_2), 4.58 (m, 4 H, C2-H_2 and C2′-H_2), 3.95 (t, 2 H, J = 8.3 Hz, C2″-H_2), 3.88 (s, 3 H, CO_2CH_3), 3.22 (t, 4 H, J = 8.3 Hz, C1-H_2 and C1′-H_2), 3.08 (t, 2 H, J = 8.3 Hz, C1″-H_2), 1.50 (br s, 9 H, *t*Bu); IR (KBr) ν_{max} 3426, 1700, 1618, 1508, 1342, 1140, 758 cm^{-1}; FABMS (*m*-nitrobenzyl alcohol) *m/e* 729 (M^+); FABHRMS (*m*-nitrobenzyl alcohol *m/e* 730.2939 ($C_{39}H_{39}N_9O_6$ + H^+ requires 730.3101).

Anal. Calcd for $C_{39}H_{39}N_9O_6$: C, 64.18; H, 5.39; N, 17.27. Found: C, 62.46; H, 5.09; N, 17.53.

Methyl 5-Amino-3-[[5′-amino-3′-[[5″-amino-3″-[[5‴-amino-3‴-(*tert*-butyloxycarbonyl)-1‴,2‴-dihydro-3‴*H*-pyrrolo[3‴,2‴-*e*]indol-7‴-yl]carbonyl]-1″,2″-dihydro-3″*H*-pyrrolo[3″,2″-*e*]indol-7″-yl]carbonyl]-1′,2′-dihydro-3′*H*-pyrrolo[3′,2′-*e*]indol-7′-yl]carbonyl]-1,2-dihydro-3*H*-pyrrolo[3,2-*e*]indole-7-carboxylate (7). A solution of 18 (32.5 mg, 0.022 mmol) in dry THF–DMF (2.5:1, 1.0 mL) was treated with 10% palladium on carbon (16.3 mg, 0.5 wt equiv) and placed under an atmosphere of H_2 (1 atm) at 23 °C (24 h). The reaction mixture was filtered through Celite, and the solvent was removed in vacuo. Chromatography (5 mm × 6 cm, 100% EtOAc–100% THF gradient elution) gave 7 (8.3 mg, 20.6 mg theoretical, 40%) as a dark green solid: mp > 275 °C dec (green flakes, THF); ^1H NMR (DMSO-d_6, 300 MHz) δ 11.59 (br s, 1 H, NH), 11.33 (br s, 1 H, NH), 11.25 (br s, 1 H, NH), 11.21 (br s, 1 H, NH), 7.63 (s, 1 H, C4-H), 7.61 (s, 1 H, C4′-H), 7.60 (s, 1 H, C4″-H), 7.51 (s, 1 H, C4‴-H), 7.01 (s, 1 H, C8″-H or C8‴-H), 6.98 (s, 1 H, C8″-H or C8‴-H), 6.85 (br s, 2 H, C8-H and C8′-H), 5.60–5.40 (m, 8 H, NH_2), 4.65–4.50 (m, 4 H, C2-H_2 and C2′-H_2), 4.12 (t, 2 H, J = 8.1 Hz, C2″-H_2), 3.95 (t, 2 H, J = 8.1 Hz, C2‴-H), 3.89 (s, 3 H, CO_2CH_3), 3.30–3.05 (m, 8 H, C1-H_2, C1′-H_2, C1″-H_2, and C1‴-H_2), 1.50 (s, 9 H, *t*Bu); IR (KBr) ν_{max} 3432, 2924, 1702, 1618, 1524, 1422, 1256, 1138, 1024, 762 cm^{-1}; FABMS (*m*-nitrobenzyl alcohol) *m/e* 928 (M^+); FABHRMS (*m*-nitrobenzyl alcohol) *m/e* 929.4078 ($C_{50}H_{48}N_{12}O_7$ + H^+ requires 929.3846).

Methyl 5-(Trimethylammonio)-3-(*tert*-butyloxycarbonyl)-1,2-dihydro-3*H*-pyrrolo[3,2-*e*]indole-7-carboxylate Iodide (8). A solution of $ACDPI_1$ (**4**, 50 mg, 0.15 mmol) in dry DMF (0.5 mL) was treated with $NaHCO_3$ (63 mg, 0.76 mmol, 5 equiv) and CH_3I (50 μL, 0.76 mmol, 5 equiv) and stirred vigorously at 23 °C (12 h). Additional CH_3I (50 μL, 0.76 mmol, 5 equiv) was added, and the mixture was stirred for 12 h (23 °C). The DMF was removed in vacuo, the resulting crude solid was slurried in water (2 × 3 mL), and the product was collected by centrifugation. Recrystallization from CH_3CN provided the $TACDPI_1$ (**8**, 61 mg, 75 mg theoretical, 81%) as a pale white plates: mp 160–161.5 °C dec (pale white plates, CH_3CN); ^1H NMR (CD_3CN, 300 MHz) δ 8.40 (br s, 1 H, NH), 7.93 (br s, 1 H, C4-H), 7.23 (s, 1 H, C8-H), 4.11 (t, 2 H, J = 8.7 Hz, NCH_2CH_2), 3.94 (s, 3 H, CO_2CH_3), 3.78 (s, 9 H, $N(CH_3)_3$), 3.32 (t, 2 H, J = 8.7 Hz, NCH_2CH_2), 1.55 (br s, 9 H, *t*Bu); IR (KBr) ν_{max} 3432, 3008, 2966, 1698, 1636, 1522 cm^{-1}; EIMS *m/e* (relative intensity) 373 (M^+ – I, 28), 317 (90), 273 (34), 57 (base); CIMS (isobutane) *m/e* 374 (M^+ + H – I, base); EIHRMS *m/e* 373.1998 ($C_{20}H_{28}IN_3O_4$ – I requires 373.2002).

Methyl 5-(Trimethylammonio)-3-[[5′-(trimethylammonio)-3′-(*tert*-butyloxycarbonyl)-1′,2′-dihydro-3′*H*-pyrrolo[3′,2′-*e*]indol-7′-yl]carbonyl]-1,2-dihydro-3*H*-pyrrolo[3,2-*e*]indole-7-carboxylate Diiodide (9). A solution of $ACDPI_2$ (**5**, 32.5 mg, 0.061 mmol) in dry DMF (0.6 mL) was treated with $NaHCO_3$ (102 mg, 1.23 mmol, 20 equiv) and CH_3I (60 μl, 0.92 mmol, 15 equiv) and stirred vigorously at 23 °C (32 h). The solvent was removed in vacuo, the crude residue was washed with H_2O (4 × 2.5 mL), and the product was collected by centrifugation. Crystallization from CH_3OH–Et_2O provided the $TACDPI_2$ (**9**, 15 mg, 53 mg theoretical, 28%) as a pale yellow solid. Additional material could be obtained from the mother liquors by repeated recrystallization: mp 150–152 °C dec (fine pale yellow needles, MeOH–Et_2O); ^1H NMR (CD_3CN, 300 MHz) δ 10.42 (br s, 2 H, NH), 8.87 (br s, 1 H, C4-H), 8.38 (br s, 1 H, C4′-H), 7.38 (s, 1 H, C8′-H), 7.22 (s, 1 H, C8-H), 4.70 (t, 2 H, J = 8.2 Hz, C2-H_2), 4.14 (t, 2 H, J = 8.2 Hz, C2′-H_2), 3.94 (s, 3 H, CO_2CH_3), 3.77 (s, 9 H, $N(CH_3)_3$), 3.75 (s, 9 H, $N(CH_3)_3$), 3.56 (t, 2 H, J = 8.2 Hz, C1-H_2), 3.37 (t, 2 H, J = 8.2 Hz, C1′-H_2), 1.55 (br s, 9 H, *t*Bu); IR (KBr) ν_{max} 3424, 1686, 1624, 1516 cm^{-1}; FABMS (*m*-nitrobenzyl alcohol) *m/e* (relative intensity) 743 (M^+ – I, 6), 154 (base); FABHRMS (*m*-nitrobenzyl alcohol) *m/e* 743.2402 ($C_{34}H_{44}I_2N_6O_5$ – I requires 743.2418).

Methyl 5-(Trimethylammonio)-3-[[5′-(trimethylammonio)-3′-[[5″-(trimethylammonio)-3″-(*tert*-butyloxycarbonyl)-1″,2″-dihydro-3″*H*-pyrrolo[3″,2″-*e*]indol-7″-yl]carbonyl]-1′,2′-dihydro-3′*H*-pyrrolo[3′,2′-*e*]indol-7′-yl]carbonyl]-1,2-dihydro-3*H*-pyrrolo[3,2-*e*]indole-7-carboxylate Tris(methanesulfonate) (10). A solution of $ACDPI_3$ (**6**, 24.9 mg, 0.034 mmol) and $NaHCO_3$ (57 mg, 0.68 mmol, 20 equiv) in dry DMF (0.3 mL) was treated with Me_2SO_4 (47 μl, 0.51 mmol, 15 equiv), and the resulting reaction mixture was stirred vigorously at 23 °C (48 h). The solvent was removed in vacuo, the crude residue was washed with H_2O (2 × 2.5 mL), and the dark green solid was collected by centrifugation. Recrystallization from CH_3OH provided the $TACDPI_3$ (**10**, 10.7 mg, 38 mg theoretical, 28%) as dark green flakes. Additional product could be obtained by recrystallization of the residue derived from the mother liquors: mp > 240 °C dec (dark green flakes, MeOH); ^1H NMR (DMSO-d_6, 300 MHz) δ 12.44 (br s, 2 H, two NH), 12.13 (br s, 1 H, NH), 8.89 (br s, 1 H, C4-H), 8.72 (s, 1 H, C4′-H), 8.17 (br s, 1 H, C4″-H), 7.49 (s, 2 H, C8″-H and C8′-H), 7.38 (s, 1 H, C8-H), 4.70 (t, 4 H, J = 8.3 Hz, C2-H_2 and C2′-H_2), 4.30 (t, 2 H, J = 8.3 Hz, C2″-H_2), 3.94 (s, 3 H, CO_2CH_3), 3.82 (s, 18 H, $N(CH_3)_3$), 3.78 (s, 9 H, $N(CH_3)_3$), 3.60 (t, 4 H, J = 8.3 Hz, C1-H_2 and C1′-H_2), 2.46 (t, 2 H, J = 8.3 Hz, C1″-H_2, partially obscured by H_2O peak), 2.54 (s, 9 H, $MeSO_4$), 1.52 (br s, 9 H, *t*Bu); IR (KBr) ν_{max} 3468, 2958, 2122, 1720, 1638, 1510 cm^{-1}; FABMS (DTT/DTE) *m/e* (relative intensity) 1214 (M^+ + Na), 1080 (M^+ – $MeSO_4$); FABHRMS (DDT/DTE) *m/e* 1080.4150 ($C_{50}H_{66}O_{14}N_9S_2$ requires 1080.4171).

DNA Binding Studies.[24] DNA (0.887 × 10^{-5} M) was mixed with ethidium bromide (0.444 × 10^{-5} M) in a 2:1 ratio of base-pair:ethidium in a 0.1 M Tris-HCl, 0.1 M NaCl, pH 8.0 buffer solution. The fluorescence spectrophotometer was calibrated at 23 °C to 100% F and 0% F with the DNA–ethidium buffer solution and ethidium buffer solution, respectively. The premixed DNA–ethidium solution was titrated dropwise with the agents (e.g., 0.2 mM $CDPI_3$ in DMSO, generally 0.2–0.8 mM) and incubated at 23 °C for approximately 30 min prior to each fluorescence reading. The fluorescence measurements were conducted at 545-nm excitation and 595-nm emission wavelengths with a slit opening of 20 nm. Under these conditions, $ACDPI_n$ and $TACDPI_n$ alone or in the presence of DNA did not interfere with the fluorescence measurements. The relative and absolute binding constants were determined at 50% ethidium bromide displacement as measured by a drop in fluorescence to 50%. The binding constants of ethidium bromide employed to calculate the absolute binding constants with a competitive binding model[22] were 6.5 × 10^5 M^{-1}, poly[dA]-poly[dT]; 4.5 × 10^6 M^{-1}, poly-[dG]-poly[dC]; and 9.5 × 10^6 M^{-1}, poly[d(A-T)]-poly[d(A-T)].[25]

Abbreviations: CPI, 7-methyl-1,2,8,8a-tetrahydrocyclopropa[1,2-*c*]pyrrolo[3,2-*e*]indol-4(5*H*)-one; CDPI, methyl N^3-carbamoyl-1,2-dihydro-3*H*-pyrrolo[3,2-*e*]-indole-7-carboxylate; ACDPI, 5-amino-CDPI; TACDPI, 5-(trimethylammonio)-CDPI.

Acknowledgment. This work was supported by the National Institutes of Health (CA 41986).

Supplementary Material Available: ^1H NMR of **5–10**, **15–16**, and **18** (9 pages). Ordering information is given on any current masthead page.

(24) Fluorescence measurements used in the DNA binding studies were obtained on a Perkin-Elmer MPF-44A Fluorescence Spectrophotometer. The DNA used in the binding studies was purchased from Sigma.

(25) Baguley, B. C.; Falkenhaug, E.-M. *Nucl. Acids Res.* **1978**, *5*, 161.